

Switching space-time interference cancellation for OFDM systems with unsynchronized cells

Alexandr M. Kuzminskiy
Bell Laboratories, Alcatel-Lucent
Swindon SN5 7DJ, UK
ak9@alcatel-lucent.com

Yuri I. Abramovich
Defence Science & Technology Organisation
PO Box 1500, Edinburgh SA 5111, Australia
Yuri.Abramovich@dsto.defence.gov.au

Abstract—Adaptive interference cancellation is addressed in an asynchronous orthogonal frequency-division multiplexing (OFDM) system with a frame containing a number of temporally distributed pilot symbols, e.g., as in the IEEE 802.16-2004 standard. A non-stationary symbol-by-symbol switching technique is proposed that is based on banks of the second-order statistics semi-blind solutions with on-line algorithm selection using a higher-order statistics criterion. Three banks of algorithms are formulated. Efficiency of the proposed algorithms is compared to the conventional stationary solution by means of simulations including a WIMAX (Worldwide Interoperability for Microwave Access) environment.

I. INTRODUCTION

Interference at the radio receiver is a key source of degradation in quality of service as experienced in wireless communication systems. Multiple-antenna interference cancellation (IC) at the receiver has been a subject of a great deal of research in different application areas including wireless communications, e.g., [1] - [4] and many other articles. In wireless communication systems, unsynchronized transmissions in neighboring cells leads to a non-stationary asynchronous co-channel interference (CCI) scenario, where some of the interference components may not overlap with the training data of the desired signal ([5], [6], and others). Conventional training-based space-time IC techniques may not be efficient in this situation. One example of such a scenario is interference mitigation on the uplink of a cellular WIMAX-compliant system based on the IEEE 802.16-2004 [7] or ETSI HiperMAN [8] standards addressed in [9].

A second-order statistics adaptive semi-blind (SB) algorithm for asynchronous CCI cancellation is proposed and studied in [6]. It is based on regularization of the conventional training-based least squares (LS) solution by means of the weighted covariance matrix estimated over the data interval. It is shown in [6] that its performance in typical asynchronous CCI scenarios is close to the performance of an averaged non-asymptotic maximum likelihood (ML) benchmark jointly estimated over both the training and working data intervals.

It is pointed out in [5] that temporally spreading the training symbols over the data slot (distributed training) could significantly simplify cancellation of the asynchronous CCI because it increases probability of overlapping between CCI and the training data. A simple case with one CCI component is

addressed in [5] by means of the SB algorithm with projections to the finite alphabet (FA).

A non-stationary IC solution is presented in [9] in the case of a flat fading assumption for the CCI, where the interference statistic can be estimated on-line using averaging over the tracking sub-carriers of an OFDM system.

In this paper, non-stationary semi-blind IC is addressed in a distributed training scenario with a number of interference components that propagate similarly to the desired signal channels. This scenario is relevant for unsynchronized WIMAX-based cellular [9] and backhaul [11] networks.

The main idea is to exploit channel correlation between adjacent sub-carriers and apply OFDM symbol-by-symbol (group of sub-carriers-by-group of sub-carriers) switching processing over the current OFDM symbol and the surrounding pilot symbols. Switching is applied over a bank of the SB algorithms defined for each possible scenario. Distance from the FA is used as a switching criterion. Three banks of the SB estimators are designed and studied in typical propagation conditions demonstrating significant performance improvement compared to the conventional stationary least squares (LS) algorithm. Further analysis of the proposed non-stationary interference cancellation techniques is given in [10] by means of comparison to the non-asymptotic ML benchmark.

An asynchronous non-stationary interference scenario is analyzed in Section 2. Data model and problem formulation are given in Section 3. Non-stationary switching solutions are developed in Section 4. The simulation results are presented in Section 5. The conclusions are summarized in Section 6.

II. INTERFERENCE SCENARIO

We consider an uplink of an unsynchronized cellular wireless network illustrated in Fig. 1 [9]. Shaded cells in Fig. 1 represent the first ring of interference for reception of user U_0 by base station BS_0 . Users in the interfering cells transmit signals (CCI for reception of the signal of interest) to their base stations $BS_1 - BS_3$. All the users transmit similar data frames according to the IEEE 802.16-2004 standard [7]. A data frame is illustrated in Fig.2. It consists of L bursts of N_{symb} OFDM symbols including preamble, which contains a training sequence for synchronization and channel estimation, data, and pilot sub-carriers. All the signals in Fig. 1 propagate through similar multipath channels and are received at base

station BS₀. It is assumed that only one transmission per cell is allowed.

As long as all users transmit similar frames and only one transmission per cell is allowed, each frame of the desired signal may be affected by 6 CCI components in a 3 interfering cell network shown in Fig. 1.

A corresponding interference scenario is shown in Fig. 3. A number of the training intervals in a frame of the desired signal creates a special form of a distributed training scenario. Taking into account that our target is a fixed wireless network [7] we assume that propagation channels are stationary over the whole data frame. Nevertheless, the interference scenario in Fig. 3 is non-stationary because of the random switching moments between different interference components.

It is worth emphasizing that the interference scenario illustrated in Fig. 3 actually represents a more general class of scenarios than the uplink cellular case. Particularly, it includes a WIMAX-based backhaul network, e.g., addressed in [11].

It is clear that the non-stationary interference scenario in Fig. 3 requires non-stationary interference cancellation at the receiver. Indeed, conventional stationary training-based processing (one weight vector estimated over all the preambles shown in Fig. 3 is used for data recovery over all the bursts) cannot be effective in this scenario because all 4 preambles in this example are affected by 6 interference components, but only 3 of them are present at any time instant during the desired signal data frame.

The main feature of this scenario is that different data intervals may require different IC algorithms. For example, for some intervals the sets of the CCI components may be different compared to the surrounding training intervals. These types of data intervals will be referred to as intervals with indirect training. Particularly, training interval T₁ in Fig. 3 overlaps with CCI 1, 3, and 5, T₂ overlaps with CCI 2, 4, and 5, but the data interval D₂ with indirect training contains different set of CCI 2, 3, and 5. All other data intervals in Fig. 3 can be associated with one of the training intervals with the same set of interference components.

III. DATA MODEL AND PROBLEM FORMULATION

In the beginning, we consider a narrowband data model for a group of sub-carriers assuming the same propagation channel for all sub-carriers in a group. Then, the developed algorithms will be exploited in the OFDM case in Section 5 based on a group-interpolation technique [12].

The signal received by an antenna array of K elements can be expressed as follows:

$$\mathbf{X}(n) = \mathbf{h}\mathbf{s}(n) + \sum_{m=1}^M \mathbf{g}_m \mathbf{u}_m(n) + \mathbf{Z}(n), \quad (1)$$

where $n = 1, \dots, N$ is the time index, N is the number of symbols, $\mathbf{X}(n) = [\mathbf{x}_1(n), \dots, \mathbf{x}_{N_{\text{gr}}}(n)]$ is the $K \times N_{\text{gr}}$ matrix of the received signals for a group of N_{gr} sub-carriers of the n th symbol, $\mathbf{x}_p(n)$ is the $K \times 1$ vector of the received signals for the p th sub-carrier, $\mathbf{s}(n) =$

$[s_1(n), \dots, s_{N_{\text{gr}}}(n)]$ is the $1 \times N_{\text{gr}}$ vector of the desired signals, $\mathbf{E}\{\mathbf{s}^*(n)\mathbf{s}(n)\} = \mathbf{I}_{N_{\text{gr}}}$, $\mathbf{E}\{\mathbf{s}^*(q)\mathbf{s}(g)\} = 0$, $q \neq g$, $\mathbf{u}_m(n) = [u_{m1}(n), \dots, u_{mN_{\text{gr}}}(n)]$ are the $1 \times N_{\text{gr}}$ vectors of the $m = 1, \dots, M$ independent CCI components,

$$\mathbf{E}\{\mathbf{u}_m^*(q)\mathbf{u}_m(g)\} = \begin{cases} p_m \mathbf{I}_{N_{\text{gr}}} & \text{for } q = g \in \mathcal{N}_m \\ 0 & \text{for all other } q \text{ and } g \end{cases}, \quad (2)$$

\mathcal{N}_m is the appearance interval for the m th CCI component, \mathbf{h} and \mathbf{g}_m are the $K \times 1$ complex vectors modeling linear propagation channels for the desired signal and interference, $\mathbf{Z}(n)$ is the $K \times N_{\text{gr}}$ matrix of AWGN with variance p_0 , $\mathbf{E}\{\cdot\}$, $(\cdot)^*$, and \mathbf{I}_J denote expectation, complex conjugate and the $J \times J$ unity matrix. All propagation channels are assumed to be stationary over the whole data frame and independent for different antenna elements and frames. As in Section 2, a data frame consists of L slots of N_{sym} symbols and the training symbol $\mathbf{s}_t = [s_{t1}, \dots, s_{tN_{\text{gr}}}]$ is located in the beginning of each slot.

We assume that reception is perfectly synchronized with the desired signal, the interference appearance intervals \mathcal{N}_m , $m = 1, \dots, M$ are not known at the receiver, sufficient second-order statistics can be estimated on a symbol-by-symbol basis, i.e., $N_{\text{gr}} > K$, and the number of antenna elements exceeds the total number of signals at any time instant, i.e., $K > M/2 + 1$.

A signal estimate can be found as the output of a non-stationary spatial filter

$$\hat{\mathbf{s}}(n) = \mathbf{w}^*(n)\mathbf{X}(n), \quad (3)$$

where $\mathbf{w}(n)$ is a $K \times 1$ weight vector for the n th symbol.

The minimum mean square error (MMSE) weight vector can be defined as follows:

$$\mathbf{w}_{\text{MMSE}}(n) = \mathbf{R}^{-1}(n)\mathbf{h}, \quad (4)$$

where $\mathbf{R}(n) = \mathbf{E}\{\mathbf{X}(n)\mathbf{X}^*(n)\}$ is the covariance matrix of the received signal for the n th symbol. For example, in the scenario in Fig. 3 for the indirect training interval $n \in D_2$, we have $\mathbf{R}(n) = \mathbf{h}\mathbf{h}^* + p_2\mathbf{g}_2\mathbf{g}_2^* + p_3\mathbf{g}_3\mathbf{g}_3^* + p_5\mathbf{g}_5\mathbf{g}_5^* + p_0\mathbf{I}_K$.

A basic problem is to estimate $\mathbf{w}_{\text{MMSE}}(n)$ using the known training sequence and all the available training T_l and stationary data intervals D_i. Taking into account that the interference appearance intervals \mathcal{N}_m and, hence, the stationary data intervals D_i are not known at the receiver, in this paper we address a simplified problem of estimation of $\mathbf{w}_{\text{MMSE}}(n)$ using symbol-based second-order statistics. This simplification allows us to overcome a difficult problem of \mathcal{N}_m estimation, although, it may compromise potential performance.

Thus, the problem is to estimate $\mathbf{w}_{\text{MMSE}}(n)$ using the known training sequence and symbol-based second-order statistics

$$\hat{\mathbf{R}}_t = N_{\text{gr}}^{-1} \mathbf{X}(1+(l-1)N_{\text{sym}})\mathbf{X}^*(1+(l-1)N_{\text{sym}}), \quad l = 1, \dots, L, \quad (5)$$

$$\hat{\mathbf{r}}_t = N_{\text{gr}}^{-1} \mathbf{X}(1+(l-1)N_{\text{sym}})\mathbf{s}^*(1+(l-1)N_{\text{sym}}), \quad l = 1, \dots, L, \quad (6)$$

$$\hat{\mathbf{R}}(n) = N_{\text{gr}}^{-1} \mathbf{X}(n)\mathbf{X}^*(n),$$

$$n = 2 + (l - 1)N_{\text{sym}}, \dots, lN_{\text{sym}}, l = 1, \dots, L - 1, \quad (7)$$

and compare performance to the conventional stationary training-based LS solution estimated over all the available training statistics¹

$$\hat{\mathbf{w}}_{\text{LS}} = \left(\sum_{l=1}^L \hat{\mathbf{R}}_{t_l} \right)^{-1} \sum_{l=1}^L \hat{\mathbf{r}}_{t_l}. \quad (8)$$

IV. SWITCHING NON-STATIONARY SOLUTION

The main idea of a symbol-by-symbol (group of sub-carriers-by-group-of-sub-carriers) switching (SSS) algorithm is to recover each symbol by means of a number of algorithms corresponding to different possible CCI scenarios with consecutive selection of the best estimates using some higher-order statistic criterion, e.g., distance from the FA. The SSS solution can be summarized as follows:

$$\hat{\mathbf{s}}(n) = \hat{\mathbf{s}}_{g_0}, \quad (9)$$

$$\hat{\mathbf{s}}_g(n) = \hat{\mathbf{w}}_g^*(n) \mathbf{X}(n), \quad (10)$$

$$g_0 = \arg \min_{g=1, \dots, G} \text{dist}_{\text{FA}} \{ \hat{\mathbf{s}}_g(n) \}, \quad (11)$$

$$\text{dist}_{\text{FA}} \{ \hat{\mathbf{s}}_g(n) \} = \sum_{q=1}^{N_{\text{gr}}} \min_{e=1, \dots, E} (|a_e - \hat{s}_{gq}(n)|), \quad (12)$$

where $\hat{\mathbf{s}}_g(n)$ is the g th signal candidate, G is the number of estimation algorithms, and a_e is the e th symbol of the FA of E symbols.

Distance from the FA is a natural criterion for communications signals. For example, it is used in [13] for on-line selection of the stationary burst-based estimates. In the considered environment, the main problem is to find a set of algorithms for estimation of signal candidates $\hat{\mathbf{s}}_g(n)$. To do that, we need to analyze all the possible scenarios that can be met on symbol-by-symbol basis²

Let us consider the 3 interfering cell scenario shown in Fig. 1 and 3 and define all the possible interference scenarios for a data symbol and the left and right surrounding training symbols as illustrated in Fig. 4. All 6 possible different scenarios are presented in Fig. 5. All other possible scenarios can be transformed to one of the cases shown in Fig. 5 by means of renumbering the interference components and exchanging the training intervals. For example, in Fig. 3, all the symbols from D_1 and D_3 belong to Scenario 3, from D_2 to Scenario 5, from D_4 and D_5 to Scenario 2, and from D_6 to Scenario 1.

¹As indicated in (7), for simplification we estimate data symbols for the first $L - 1$ slots in a frame. Edge effects for the last slot in a frame can be addressed by a similar way.

²In the narrowband data model we assume that switching moments are synchronized on a symbol basis. In an unsynchronized OFDM systems this means that at this stage we ignore symbols affected by switching moments. The number of such symbols is low compared to the total number of estimated symbols, which allows us to expect that they will not significantly affect the overall performance. Furthermore, in our OFDM simulations in Section 5, we apply the developed algorithms for all the symbols in a frame and demonstrate acceptable performance degradation for the symbols affected by the asynchronous switching moments.

A. Case studies

Scenario 1: Scenario 1 represents a conventional case of the synchronous CCI. It is shown in [14], that in this case the conventional LS solution estimated over the whole training interval

$$\hat{\mathbf{w}}_{\text{LS}} = \left(\hat{\mathbf{R}}_{t\text{-left}} + \hat{\mathbf{R}}_{t\text{-right}} \right)^{-1} \left(\hat{\mathbf{r}}_{t\text{-left}} + \hat{\mathbf{r}}_{t\text{-right}} \right) \quad (13)$$

is very close the ML solution and cannot be significantly improved by means of using the data interval even if it is indefinitely long. Thus, we select the LS estimator (13) for Scenario 1.

Scenarios 2, 3, and 4: Scenarios 2, 3, and 4 are similar because all of them contain the (right) training symbol with the same set of the CCI components as the data symbol. Thus, a natural choice for these Scenarios could be the LS algorithm based on the corresponding training symbol

$$\hat{\mathbf{w}}_{\text{LS-right}} = \hat{\mathbf{R}}_{t\text{-right}}^{-1} \hat{\mathbf{r}}_{t\text{-right}}. \quad (14)$$

It is worth emphasizing that generally, the LS solution (14) can be improved by means of a semi-blind processing over the data and training symbols depending on particular scenario parameters such as K , N_{gr} , p_q , and p_0 .

Scenario 5: As was already mentioned, Scenario 5 is significantly different compared to Scenarios 1 - 4 because there are no training samples containing the same CCI components as the data symbol. This means that the LS algorithm based on the left, right or both the training intervals cannot be effective in this case and semi-blind processing is required.

The simplest solution could be a regularized LS (RLS) algorithm [6] based on one of the training intervals, e.g., the right one:

$$\hat{\mathbf{w}}_{\text{RLS-right}} = \left[(1 - \delta) \hat{\mathbf{R}}_{t\text{-right}} + \delta \hat{\mathbf{R}} \right]^{-1} \hat{\mathbf{r}}_{t\text{-right}}. \quad (15)$$

where $0 < \delta < 1$ is the regularization coefficient that controls the cancellation ability of the interference component that is present in the data interval and not present in the right training interval (CCI 3 in this particular case) and performance degradation because of distortion of the LS solution required for cancellation of CCI 2 and 5. Efficiency of the regularized algorithm and selection of the regularization coefficient is studied in [6], [15] in the general asynchronous CCI scenario.

The regularized algorithm (15) can be applied in the general case with a number of new interference components in the data interval compared to the training data. In the particular Scenario 5, where only one new CCI component appears in the data interval, specific semi-blind algorithms could be exploited.

One option is to use the data samples for cancellation (“cleaning”) of the interference components at the training symbols that are not present in the data interval. This can be done by means of a two-stage adaptive noise canceller (ANC) [16], [17] as illustrated in Fig. 6.

At the first stage, a spatial filter estimated over the data samples that cancels all the interference components and

the desired signal, is applied over the training symbols to obtain the signals correlated to the interference components not presented on the data interval:

$$\mathbf{y}_t = \mathbf{u}_{\min}^*(\hat{\mathbf{R}})\mathbf{X}_t, \quad (16)$$

where \mathbf{y}_t is the $1 \times N_{\text{gr}}$ output vector at the first ANC stage calculated for the left (t-left) and right (t-right) training intervals, $\mathbf{u}_{\min}(\mathbf{B})$ is the eigenvector corresponding to the minimum eigenvalue of matrix \mathbf{B} .

Then, the ‘‘cleaned’’ training samples can be obtained as follows:

$$\tilde{\mathbf{x}}_{tk} = \mathbf{x}_{tk} - \hat{f}_{tk}\mathbf{y}_t, \quad k = 1, \dots, K, \quad (17)$$

where \mathbf{x}_{tk} is the k th row of the matrix \mathbf{X}_t and

$$\hat{f}_{tk} = \frac{\mathbf{y}_t \mathbf{x}_{tk}^*}{\mathbf{y}_t \mathbf{y}_t^*}. \quad (18)$$

Eventually, the ‘‘cleaned’’ sufficient statistics $\tilde{\mathbf{R}}_t = N_{\text{gr}}^{-1} \tilde{\mathbf{X}}_t \tilde{\mathbf{X}}_t^*$ and $\tilde{\mathbf{r}}_t = N_{\text{gr}}^{-1} \tilde{\mathbf{X}}_t \mathbf{s}_t^*$, where $\tilde{\mathbf{X}}_t = [\tilde{\mathbf{x}}_{t1}^T, \dots, \tilde{\mathbf{x}}_{tK}^T]^T$, can be used similarly to (13) instead of the original training statistics $\hat{\mathbf{R}}_t$ and $\hat{\mathbf{r}}_t$ to get the semi-blind solution:

$$\hat{\mathbf{w}}_{\text{SB}} = \left(\tilde{\mathbf{R}}_{t\text{-left}} + \tilde{\mathbf{R}}_{t\text{-right}} \right)^{\#} \left(\tilde{\mathbf{r}}_{t\text{-left}} + \tilde{\mathbf{r}}_{t\text{-right}} \right), \quad (19)$$

where $(\cdot)^{\#}$ is the pseudoinverse operation, which is used instead of the conventional inversion because of the reduced rank of the corresponding matrices after the ‘‘cleaning’’ operation.

A detailed study of Scenario 5 is presented in [18].

Scenario 6: Scenario 6 is similar, but more difficult compared to Scenario 5. The difference is that one of the training symbols (the left one in Fig. 5) is affected by two CCI components not presented on the other intervals. The regularized solution (15) and its natural ‘‘cleaned’’ modification, i.e., the regularized SB (RSB) algorithm

$$\hat{\mathbf{w}}_{\text{RSB-right}} = \left[(1 - \delta)\tilde{\mathbf{R}}_{t\text{-right}} + \delta\hat{\mathbf{R}} \right]^{-1} \tilde{\mathbf{r}}_{t\text{-right}}, \quad (20)$$

can be applied in this case.

B. Algorithm banks

Now, we have the algorithms to apply in all the situations that may appear in the general scenario shown in Fig. 3. Taking into account that Scenarios 2-4, and 6 are asymmetrical in terms of the left/right training intervals, we need to include both left and right versions of the corresponding estimators to the algorithm banks to be used by the SSS algorithm (9) - (12).

The first bank can be formed from the advanced SB algorithms presented in Section 4.A:

- *Bank 1*
 1. \mathbf{w}_{LS} (LS estimated over both the training intervals as in (13)),
 2. $\mathbf{w}_{\text{LS-left}}$ (LS estimated over the left training interval similarly to (14)),
 3. $\mathbf{w}_{\text{LS-right}}$ (LS estimated over the right training interval as in (14)),
 4. \mathbf{w}_{SB} (SB estimated over both the available intervals

as in (19)),

5. $\mathbf{w}_{\text{RSB-left}}$ (RSB estimated over the left training and data intervals similarly to (20)),
6. $\mathbf{w}_{\text{RSB-right}}$ (LS estimated over the right training and data intervals as in (20)).

Algorithm 1 takes care of Scenario 1, Algorithms 2 and 3 deal with Scenarios 2 - 4, Algorithm 4 address Scenario 5, and Algorithms 5 and 6 are required for Scenario 6. The SSS algorithm based on Bank 1 will be referred to as the semi-blind SSS estimator (SBSSS).

As was noted in Section 4.A, the conventional LS solution regularized by means of the data covariance matrix, could be applied in all the considered cases, possibly, with some performance degradation compared to LS in Scenarios 1 - 4 and to SB and RSB in Scenarios 5 and 6. Thus, simplified banks of algorithms can be formed as follows:

- *Bank 2*
 1. \mathbf{w}_{LS} (LS estimated over both the training intervals as in (13)),
 2. $\mathbf{w}_{\text{RLS-left}}$ (regularized LS estimated over the left training and data intervals similarly to (15)),
 3. $\mathbf{w}_{\text{RLS-right}}$ (LS estimated over the right training and data intervals as in (15)).

The SSS algorithm based on Bank 2 will be referred to as the regularized SSS estimator (RSSS).

Further simplification can be made by removing Algorithm 1 from Bank 2, taking into account that one of the training intervals in Scenario 1 contains all the CCI components present in the data interval. The SSS algorithm based on Bank 2 without Algorithm 1 will be referred to as the simplified regularized SSS estimator (SRSSS).

V. SIMULATION RESULTS

A. Narrowband case

We simulated a 5-element antenna array ($K = 5$) and 3-cell scenario illustrated in Fig. 1 and 3. The desired signal and interference are generated as independent streams of random symbols $(\pm 1 \pm j)/\sqrt{2}$. All propagation channels are simulated as independent complex Gaussian vectors with unit variance and zero mean. Signal-to-interference ratio SIR=0 dB is assumed in all narrowband simulations. The LS, SBSSS, RSSS, and SRSSS algorithms are compared by means of bit error rate (BER) performance estimated over 10^4 trials with independent channel and data realizations.

The BER performance is given in Fig. 7 for different $N_{\text{gr}} = [8, 16, 24]$ and fixed $\delta = 0.2$. Comparison of the simulation results show the following:

- As expected, all the considered non-stationary switching algorithms significantly outperform the conventional LS solution.
- The SBSSS algorithm demonstrates the best results for all the considered group sizes.
- The simplified RSSS and SRSSS algorithms are very close to SBSSS for $N_{\text{gr}} = [16, 24]$, but they demonstrate significant performance degradation for $N_{\text{gr}} = 8$, especially for SRSSS.

Fig. 8 illustrates the regularization effect on SBSSS, RSSS, and SRSSS for SNR=14 dB and different N_{gr} . One can see that the simplified RSSS and SRSSS are more sensitive to selection of the regularization parameter δ compared to SBSSS, which requires regularization only in Scenario 6. Generally, the BER functions on δ are not sharp. So, in practice, the regularization parameter can be easily selected in the desired area.

B. OFDM case

Taking into account that RSSS is significantly simpler than SBSSS, we select it for investigation in the OFDM environment.

The main simulation assumptions are as follows:

- IEEE 802.16-2004 slot structure: 256 sub-carriers, cyclic prefix of 32 samples, preamble of 128 sub-carriers, 8 pilot sub-carriers, 192 data sub-carriers,
- 5.25 GHz central frequency, 20 MHz bandwidth,
- QPSK signaling, convolutional coding with 1/2 code rate,
- 10 OFDM symbols in a slot, 4 slots in a frame,
- 1728 uncoded bits in a slot, 6912 uncoded bits in a frame,
- 14.4 μ s OFDM symbol, 144 μ s slot, and 576 μ s frame duration,
- WINNER propagation channels D1/LOS [19],
- 2λ separation between 5 receive antennas,
- 3 interfering cells, 300 m cell size,
- 30 dBm transmit power, -92 dBm noise power.

The simplification assumptions are as follows: ideal (linear) front-end-filters; zero frequency offset; perfect receiver synchronization for the desired signal; frame-stationary propagation channels.

Fig. 9 presents the BER and packet error rate (PER) performance for the LS and RSSS algorithms depending on the number of groups of sub-carriers for the desired signal located in the edge of the cell [300,300] m and the interference sources randomly located in the corresponding CCI cells shown in Fig. 1. All 200 working sub-carriers are grouped almost uniformly. For example, in the 12-group case we use the following group-size distribution: [17,17,17,17,16,16,16,16,17,17,17,17]. Additional to the LS and RSSS results, the maximum ratio combining (MRC) performance is shown in Fig. 9 for comparison with the no IC case. The performance is estimated over 1000 independent trials.

From Fig. 9, one can see that the proposed non-stationary RSSS algorithm significantly outperforms the conventional LS estimator. Particularly, in the considered scenario, RSSS demonstrates almost 4 times PER gain compared to LS in the best case of 12 groups of sub-carriers. The optimal value of the number of groups reflects a trade off between the channel approximation accuracy and the available amount of data for estimation of the weights.

The dashed BER curves in Fig. 9 represent the performance estimated over 3 OFDM symbols per frame that correspond to the CCI switching moments. As was mentioned in Section 4, the CCI scenarios may be more complicated for these moments, but that was not taken into account for algorithm

development because of the low number of such moments in a frame. Indeed, some performance degradation can be observed for such symbols for both LS and SRSSS. Nevertheless, SRSSS still outperforms LS and the overall effect of such symbols is negligible.

Similar results to Fig. 9 are obtained for different propagation channels and cell configurations.

VI. CONCLUSIONS

The adaptive non-stationary interference cancellation technique has been proposed for an asynchronous OFDM system with a frame containing a number of temporally distributed pilot symbols, e.g., as in the IEEE 802.16-2004 standard. The symbol-by-symbol switching algorithms have been developed that are based on banks of the second-order statistics semi-blind solutions with on-line algorithm selection using a distance from the finite alphabet. It has been demonstrated by means of simulations in a WIMAX environment that the proposed regularized symbol-by-symbol switching algorithm significantly outperforms the conventional stationary pilot-based estimator.

ACKNOWLEDGEMENT

Part of this work has been performed with financial support from the IST FP6 MEMBRANE project.

REFERENCES

- [1] A. Paulraj, C. B. Papadias, "Space-time processing for wireless communications," IEEE Signal Processing Magazine, vol. 14, no. 6, pp. 49-83, Nov. 1997.
- [2] A. M. Kuzminskiy, "Finite amount of data effects in spatio-temporal filtering for equalization and interference rejection in short burst wireless communications," Signal Processing, vol. 80, no. 10, pp. 1987-1997, Oct. 2000.
- [3] J. G. Andrews, "Interference cancellation for cellular systems: A contemporary overview," IEEE Wireless Communications, vol. 12, n. 2, pp. 19-29, Apr. 2005.
- [4] D. Astely, B. Ottersten, "Spatiotemporal interference rejection combining," in Smart Antennas - State of the Art, T. Kaiser, A. Bourdoux, H. Boche, J. Fonollosa, J. B. Andersen, W. Utschick, Eds., Hindawi, 2005.
- [5] C. Martin, B. Ottersten, "On robustness against burst unsynchronized co-channel interference in semi-blind detection," in Proc. 34th Asilomar Conf. Sig., Syst. and Comp., vol. 2, pp. 946-450, Nov. 2000.
- [6] A. M. Kuzminskiy, Y. I. Abramovich, "Second-order asynchronous interference cancellation: regularized semi-blind technique and non-asymptotic maximum likelihood benchmark," Signal Processing, vol. 86, no. 12, pp. 3849-3863, Dec. 2006.
- [7] IEEE 802.16-REVd/D5-2004, "IEEE Standard for Local and Metropolitan Area Networks - Part 16: Air Interface for Fixed Broadband Wireless Access Systems," May 2004.
- [8] ETSI, "Broadband Radio Access Networks (BRAN); HIPERMAN; Physical (PHY) Layer," Standard TS 102 177, 2003.
- [9] M. Nicoli, M. Sala, O. Simeone, L. Sampietro, C. Santacesaria, "Adaptive array processing for time varying interference mitigation in IEEE 802.16 systems," in Proc. PIMRC, Helsinki, Sept. 2006.
- [10] A. M. Kuzminskiy, Y. I. Abramovich, "Non-stationary multiple-antenna interference cancellation for unsynchronized OFDM systems with distributed training," in Proc. ICASSP, Las Vegas, Apr. 2008.
- [11] MEMBRANE Deliverable D4.1.2, "IA/MIMO-enabled techniques and reconfigurable routing," July 2007, <http://www.ist-membrane.org>
- [12] D. Bartolome, X. Mestre, A. I. Perez-Neira, "Single input multiple output techniques for Hiperlan/2," in Proc. IST Mobile Communications Summit, Barcelona, Sept. 2001.
- [13] A. M. Kuzminskiy, D. Hatzinakos, "Semi-blind estimation of spatio-temporal filter coefficients based on a training-like approach", IEEE Signal Processing Letters, vol.5, n.9, pp.231-233, Sept. 1998.
- [14] Y. I. Abramovich, A. M. Kuzminskiy, "On correspondence between training based and semi-blind second-order adaptive techniques for mitigation of synchronous CCI," IEEE Transactions on Signal Processing, vol. 54, no. 6, pp. 2347-2351, June 2006.

- [15] A. M. Kuzminskiy, Y. I. Abramovich, "Adaptive asynchronous CCI cancellation: selection of the regularization parameter for regularized semi-blind technique," in Proc. SPAWC, Cannes, July 2006.
- [16] W. A. Gardner, B. G. Agee, "Two-stage adaptive noise cancellation for intermittent signal applications," IEEE Trans. Inf. Theory, vol. 26, no. 12, pp. 69-98, 1980.
- [17] A. M. Kuzminskiy, "A modified adaptation algorithm for one class of noise compensator," Radioelectronics and Communications Systems, vol. 30, no. 4, pp. 18-22, 1987.
- [18] A. M. Kuzminskiy, Y. I. Abramovich, "Semi-blind interference cancellation with distributed training," in Proc. EUSIPCO, Poznan, Sept. 2007.
- [19] WINNER Deliverable D5.4, V1.4, "Final report on link level and system level channel models," 2005, <http://www.ist-winner.org>

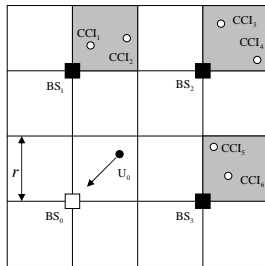


Fig. 1. Uplink layout for a wireless cellular system.

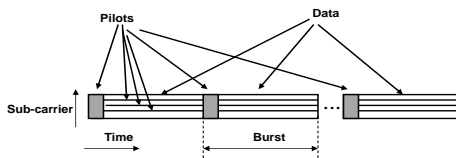


Fig. 2. WIMAX uplink frame structure.

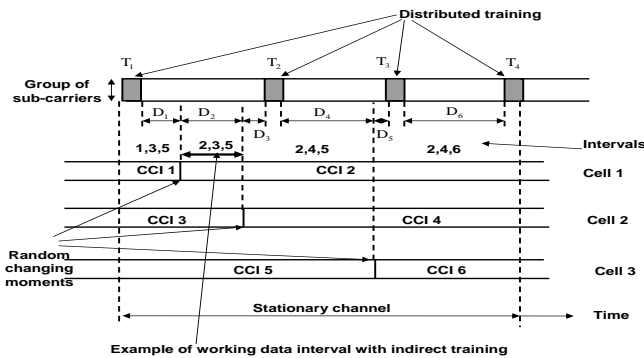


Fig. 3. Asynchronous scenario for 3 interfering cells.

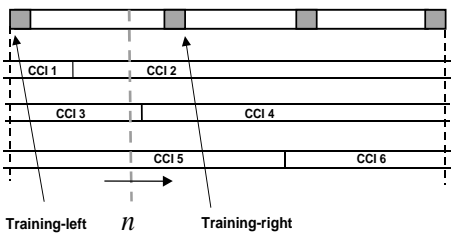


Fig. 4. Symbol-by-symbol temporal scanning.

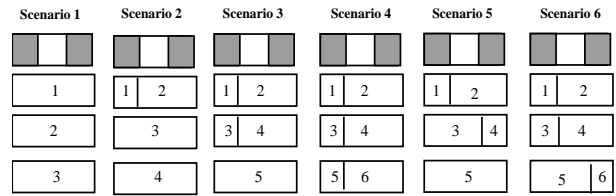


Fig. 5. Symbol-by-symbol scenarios for 3 interfering cells.

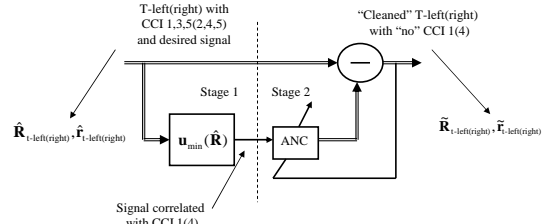


Fig. 6. Two-stage adaptive noise canceller for Scenario 5.

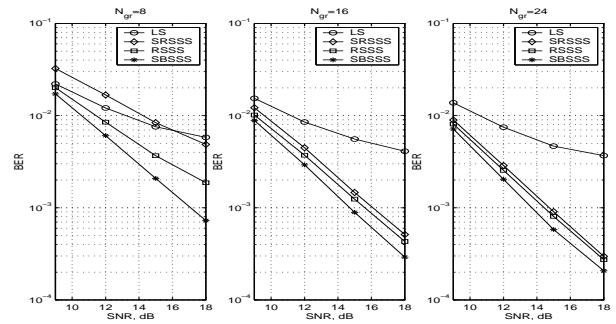


Fig. 7. BER performance in the general scenario.

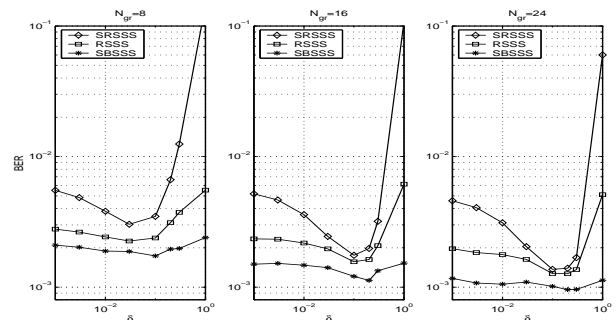


Fig. 8. Regularization effect on SBSS, RSS, and SRSS for SNR=14 dB.

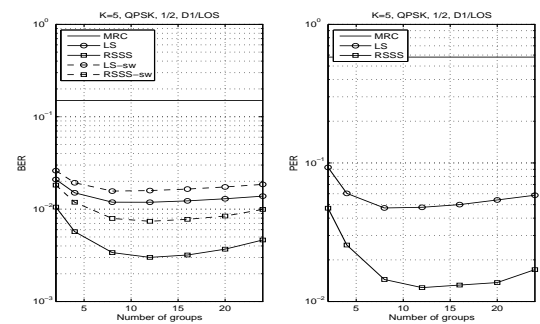


Fig. 9. OFDM results for the D1/LOS channel and 300m cell.